

# Contact indentation of marine composites

L. S. Sutherland and C. Guedes Soares

## Abstract

Quasi-static indentation tests on low fibre-volume, hand-produced, E-glass/polyester 'marine' laminates have been performed. A Hertzian contact law fitted well the initial response. Considerable material variability was seen in the Hertzian behaviour of the woven roving tests. The presence of an irregular resin-rich surface was influential at initial contact and was thought to reduce the contact stiffness for smaller diameter indenters. At higher loads the response became linear as damage became significant. The transition to linear behaviour is thought to be due to delamination. Good correlation of the transition load with indenter radius was obtained using a simplified shear delamination model. Despite their significantly lower fibre-volume, chopped strand mat laminates exhibited a slightly higher contact stiffness than woven roving laminates.

## Keywords

Indentation, Hertzian contact, Delamination, E-glass/polyester laminates

## 1. Introduction

Composite materials are now the construction material of choice for pleasure craft and are increasingly used for commercial fishing and naval vessels. Generally, low fibre-volume E-glass woven roving or chopped strand mat reinforced polyester resin laminates are produced by hand. The main advantages of these 'marine composites' are that complex double-curvature forms may be easily fabricated and that they have high specific material properties and good resistance to corrosion and rot. However, these materials are very susceptible to transverse impact damage, which may be caused during construction (e.g. tool drops or when turning/moving the hull or other components) or during operation (e.g. collisions with other craft, docks or floating debris and grounding). All of these impact events may be categorised as low energy impacts.

The response of such marine composites to impact is the subject of current work by the authors [1,2]. To replicate a fairly severe case of an impact event an instrumented falling weight machine is used where a hemispherically ended impactor attached to a variable mass is dropped from a known height onto a laterally supported fully clamped target plate. A load cell between impactor and variable mass provides impact force-time data which is integrated to give the impact head displacement.

For thicker laminates a shear deflection-based model gave good correlation with the experimental impact results. However, the stiffer response of these thicker laminates leads to high local contact forces and the effects of contact indentation for these resin-rich marine composites were seen to become significant. The measured *displacement* of the impact head ( $\delta$ ) is made up of the sum of the plate *deflection* ( $w$ ) and the *indentation* ( $\alpha$ ) (see Fig. 1).

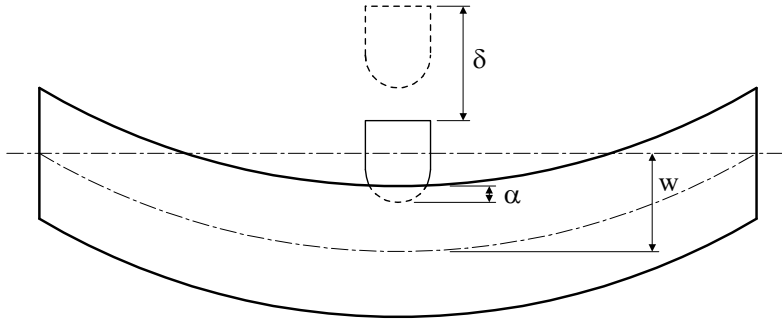


Fig. 1. Impact Force ( $P$ ), Displacement ( $\delta$ ), Indentation ( $\alpha$ ) and Deflection ( $w$ ).

Hertzian contact behaviour is usually assumed (see Section 2), but the low fibre volume fraction glass polyester laminates considered here not only deviate from the homogeneity and isotropy assumed in the theory, but for the woven roving laminates the weave size is significant in comparison to the indenter size. Also, marine composites are fabricated by hand, often under less than ideal conditions and are hence of correspondingly variable quality, usually with a resin rich surface of variable thickness and smoothness.

Further, impact testing has already shown that these materials delaminate at very low impact forces [1,2]. This delamination may occur due to shear stresses due to global deflections, or due to local contact force induced shear stresses, or to an interaction between both mechanisms. Here the delamination due to local contact forces will be studied in isolation.

Hence, since the data available in the literature exclusively concerns higher quality and fibre volume-fraction, usually unidirectional pre-preg composites, an experimental approach was taken to investigate the contact indentation behaviour of these marine composites and to provide force-indentation data for use in the impact work.

## 2. Theory

The contact force,  $P$ , is usually related to the indentation by the Hertz contact law [3], derived assuming contact between two smooth elastic, homogenous, isotropic solid bodies of revolution [4–6]:

$$P = n\alpha^{3/2} \quad (1)$$

where;

$$n = \frac{4E\sqrt{R}}{3} \quad (2)$$

and

$$\frac{1}{E} = \frac{1-\nu_1^2}{E_1} + \frac{1-\nu_2^2}{E_2} \quad ; \quad \frac{1}{R} = \frac{1}{R_1} + \frac{1}{R_2} \quad (3)$$

where the subscripts 1 and 2 refer to the indenter and target respectively,  $E$  refers to Young's modulus,  $R$  to radius and  $\nu$  is Poisson's ratio.

For the case of a flat target indented by a hemispherical indenter, Eq. (2) becomes:

$$n = \frac{4E\sqrt{R_1}}{3} \quad (4)$$

The contact radius  $a$  is given by:

$$a = \left( \frac{3PR_1}{4E} \right)^{1/3} \quad (5)$$

Despite the fact that laminated composite materials are not homogenous or isotropic it has been found experimentally that Eq. (1) also describes fairly well the contact behaviour for carbon and glass epoxy laminates [7–9]. The transverse modulus is found to be the pertinent value for  $E_2$ .

Further development of the theory for a spherical isotropic indenter and a transversely isotropic composite plate [10,11] gives:

$$n = \frac{4\sqrt{R_1}}{3\pi(K_1 + K_2)} \quad (6)$$

where  $K_1$  and  $K_2$  are constants dependant on the indenter and composite plate material properties respectively.

However, the relationships used to give  $K_2$  are very convoluted and require the input of difficult to accurately measure material properties such as through thickness shear modulus and poisons ratio, giving great scope for error.

If the target is sufficiently flexible to give large global deflections  $w$ , then ‘wrapping’ of the target around the indenter may occur. This may increase the contact area significantly, leading to a modified contact force distribution and hence force-indentation relationship. This effect has been analytically investigated for beams [12–14] and for plates [15,16].

Although the local contact stress field leading to delamination is in reality very complex, assuming a greatly simplified shear stress distribution and that the delamination occurs as the interlaminar shear strength (ILSS) is exceeded gives:

$$ILSS = \frac{P_{crit}}{2\pi ah} \quad (7)$$

where,  $P_{crit}$  is the critical load at which delamination occurs, and  $h$  is the material thickness.

Combining Eq. (5) and (7) gives:

$$P_{crit}^2 = \left( \frac{6 ILSS^3 \pi^3 h^3}{E} \right) R_1 \quad (8)$$

### 3. Experimental details

Exactly the same laminate production method as used for the impact work was used here. Panels of 30-ply  $500 \text{ gm}^{-2}$  woven roving ('WR': 50% fibres by weight or 0.35 fibre volume-fraction, average thickness 19 mm), and 20-ply  $450 \text{ gm}^{-2}$  chopped strand mat ('CSM': 33% fibres by weight or 0.2 fibre volume-fraction, average thickness 18 mm) E-glass/orthophthalic polyester panels were laminated by hand. 1, 2 and 3% by mass of accelerator, catalyst and paraffin respectively were used in an ambient temperature of between 18 and 21 degrees C, and the laminates were left to cure for at least two months at this temperature. Specimens were then cut from the panels using a diamond surrounded saw.

Quasi-static indentation testing was performed using a servo-hydraulic test machine. Force and displacement were measured using a high accuracy, misalignment error compensated load-cell (60 kN rated load) and an infinite resolution hybrid linear potentiometer respectively. Specimens were fully supported on a thick steel block and cylindrical stainless steel 'indenters' with hemispherical ends of diameter 10 mm, 20 mm and 30 mm pushed at a constant rate of displacement of 15 s/mm onto the laminate surface. As the working limit of the load cell or of the indenter was approached the direction of displacement was reversed to lift the indenter from the laminate.

It should be noted here that the fully supported plate geometry of the indentation tests differs from the clamped plate geometry of the impact tests. For the impact test geometry progressive bending of the specimens may lead to a greater contact area as the plate 'wraps around' the indenter. Some researchers, such as Tan and Sun [8], have replicated this bending and then measured the indenter movement relative to that of the back face to give the indentation. Here this approach was not thought to be advantageous for the following reasons: This bending effect is most prominent in the thinner specimens where bulging of the back face will make the method inaccurate; Indentation is most significant for the impact on stiffer, thicker specimens where the test geometry becomes very close to that of the indentation tests here; The measurement of such small differences between back-face deflections and indenter displacements is likely to lead to significant losses in accuracy; The unevenness of the surface of the laminates considered here introduces much greater deviations from the ideal geometry than those due to fully supporting the specimens.

Data was sampled at 20 Hz, and the test machine operated under displacement control, with 1 Hz low pass transducer filtering of the control loop. Unfiltered force-time and displacement data was recorded and then post filtered using a discrete Butterworth filter. It was found that low pass filtering of the data to 1 Hz optimised the removal of signal noise without the loss of any significant response features.

Repetitions of the tests were made to give an indication of the variability of the results at two levels. For each reinforcement-indenter diameter combination 3 or 6 repetitions were made on the same small specimen cut from a given part of the larger panel. Then, to investigate how the response varied across the panel, these tests were then repeated on a specimen taken either from another part of the panel or from another nominally identical panel.

#### 4. Data analysis

Although the testing was physically quite straightforward, the subsequent fitting of a Hertzian power law (c.f. Eq. (1)) was found to be extremely sensitive to the processing of the data, especially concerning the initial data points. Hence judgment of the time and displacement at which contact first occurred became critically important. The unloaded force signal was steady with a slight offset (that varied slightly between tests) and noise that always fell within  $\pm 0.05$  kN of this offset. Hence, in each case the offset was evaluated and applied to the data and then the start of contact judged to occur when the load first exceeded 0.05 kN. Importantly, this point gave the displacement to be used as the zero displacement reference for calculation of the indentation.

Many software packages will easily fit a power law directly to the force-indentation data, but it is important to realise the statistical implications of this process. It is far safer to perform a linear regression on the ln–ln data in order to inspect the fitting process. The reasons for this are best shown through the use of an illustrative example such as that given in Fig. 2.

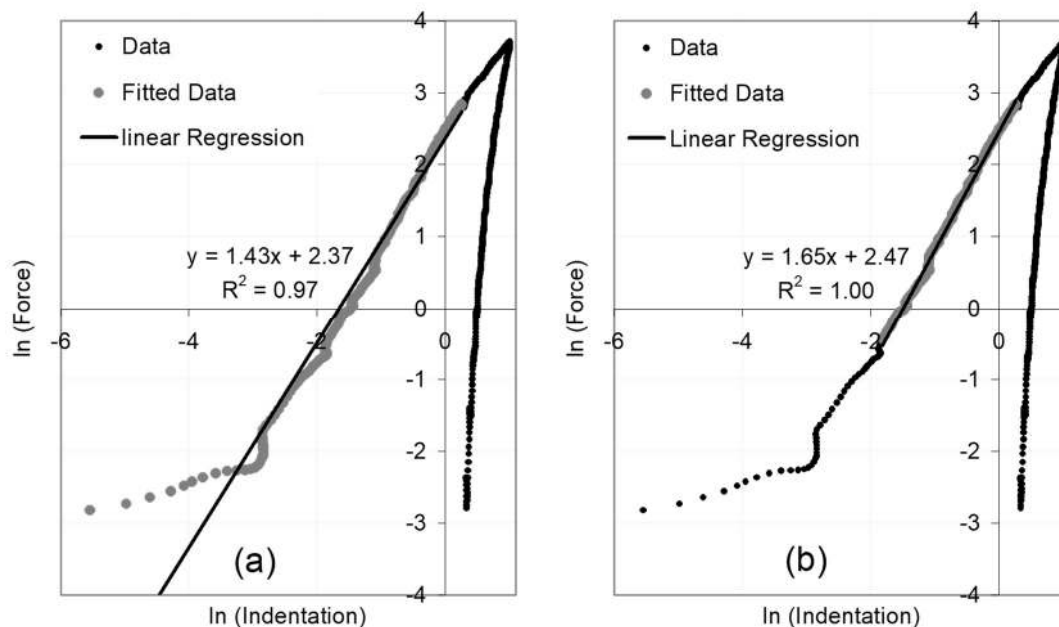


Fig. 2. Ln–Ln plots for power law fitting.

The same data is used in both plots, the difference between Fig. 2(a) and (b) is in which data has been selected to fit the linear regression. In both cases the same pertinent upper limit of the linear section is used, as discussed in the next section. However, the strong linear trend in the data does not extend to low values of force and displacement. This is due to several effects; the rough specimen surface, the presence of a resin-rich surface layer, the start of contact was assumed by necessity to be at 0.05 kN giving a small force offset, and the increased importance of measurement resolution issues at very low force and displacement values. All of these factors, when considered with respect to the range of forces and indentations considered over the test as a whole are very small, but have important consequences on the fitting of the power law.

To illustrate this, in Fig. 2(a) all initial data points were used in the regression whereas in Fig. 2(b) the lowest force and indentation data that deviates from the linear trend was excluded.

Although these initial points that deviate from the linear section constitute only a small fraction of the total number of data points, this causes a dramatic change in the fitted equations with a 15% change in the slope in this case. This is because, since the linear regression for the power law predicted in equation (1) is to be carried out on logarithmic data, 'statistical leverage' becomes important. This means that data points a long way from the centre of the range of a data set will have an disproportionately large effect on a linear regression of that data. In this case the fact that we are working in a logarithmic domain spreads the initial data points at low forces and indentations away from the centre of the data set and thus increases drastically their effect on the fitting of a linear trend.

The fact that, although slightly lower in Fig. 2(a), the 'goodness of fit' parameter  $R^2$  is very high in both cases explains why the discussion above is so important. Simply using software to fit a power law directly to the data would give a seemingly good fit, especially when viewed on a force-indentation plot. However, a residual analysis [17], if carried out, would show that the fit of Fig. 2(b) is in fact superior. Hence, although the judgement of where to start fitting the data is a potential source of subjectivity, it was consistently obvious where the linear section should begin and the initial data points were not included in the regressions reported here.

## 5. Results

A common trend was seen for all tests, at lower contact forces the contact response was of a power law form but at a certain load this gave way to linear behaviour. The results of the first set of tests on woven roving with a 20 mm diameter indenter (WR/20 mm) give a good example of this behaviour. Fig. 3 shows that separate tests on the same part of a panel show some variability, but are reasonably repeatable. The presence of damage is reflected in the permanent indentation (of around 1.5 mm in this case) at the end of the test.

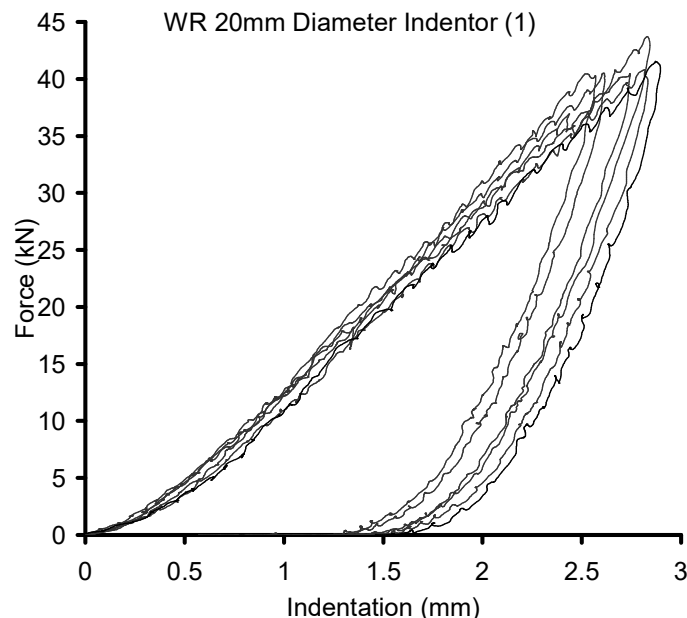


Fig. 3. Typical contact responses.

The extremely good fit of a power law followed by a linear relationship to the averaged data can be seen in Fig. 4. In fact the lowest  $R^2$  value obtained for any of the power law or linear fits was 0.992 and hence these 'goodness of fit' values are not quoted further. The

transition from Hertzian to linear behaviour was not always abrupt, often occurring over a small range of loads and is thought to occur as shear stresses gave the delamination that was seen in the tested specimens. This localised delamination due solely due to contact force is in all probability an important precursor to and/or initiator of the delamination growth due to global plate shear stresses seen in the co-current impact work [1,2].

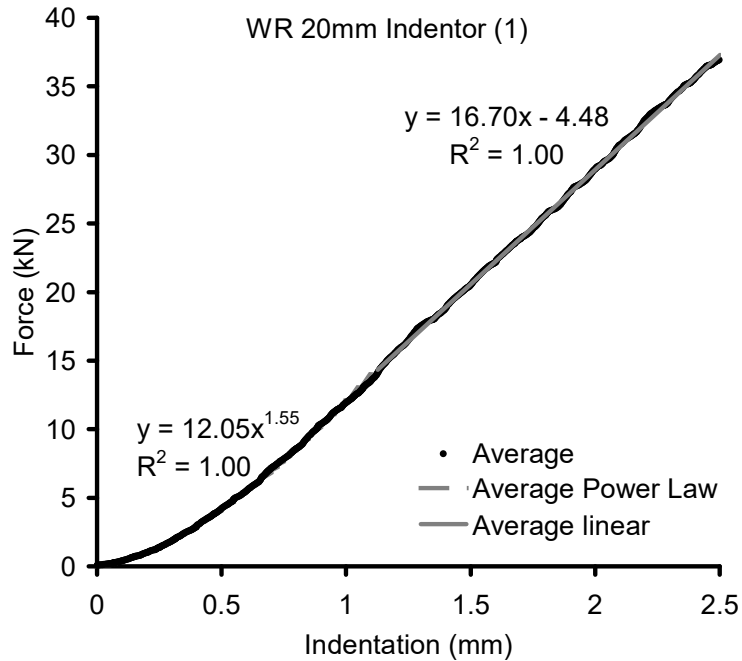


Fig. 4. Typical power law and linear response.

The deviation from the Hertzian behaviour at initial contact is much clearer from the logarithmic plot of the data as shown in Fig. 5. The reduced contact stiffness here suggests that this effect is mainly due to the irregular resin-rich surface.

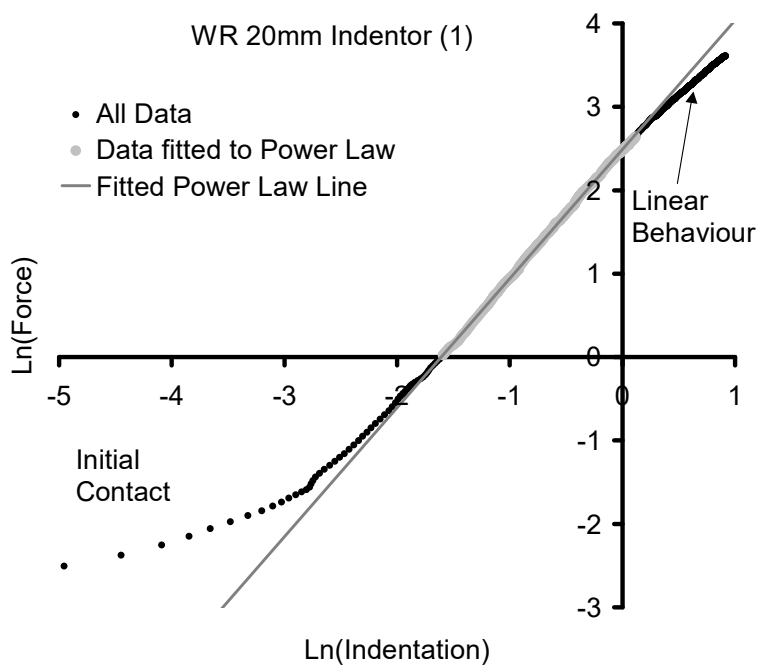


Fig. 5. Typical Ln–Ln plot.

The full results set is summarised in Table 1. For two of the WR 10 mm radius indenter data sets, tests were not carried out to sufficiently high loads for linear behaviour to occur. A measure of the variability of the results is given in terms of the coefficient of variation, but due to the relatively small number of tests in some cases these must be used as indications only. Despite the considerable deviations of these materials from the assumptions of the Hertz law as discussed in the introduction, the contact force initially varied with indentation to the power of approximately 3/2 as predicted by Eq. (1). On average the actual powers were 1.59 and 1.41 for the woven roving and chopped strand mat specimens respectively.

Reinforcement / No.	Indenter Diam.	Tests	Power Law		Transition	Linear	
			Power (kN/mm <sup>3/2</sup> )	n	Load (kN)	Slope (kN/mm)	Intercept (kN)
<b>WR 10mm (1):</b>	6	1.57 (9)	7.01 (6)	9 (8)	9.29 (9)	-1.72 (73)	
<b>WR 10mm (2):</b>	3	1.66 (2)	6.33 (8)	8 (11)	~	~	
<b>WR 10mm (3):</b>	3	1.40 (7)	9.07 (9)	8 (7)	~	~	
<b>WR 20mm (1):</b>	6	1.55 (6)	12.05 (10)	14 (18)	16.70 (7)	-4.48 (30)	
<b>WR 20mm (2):</b>	3	1.76 (3)	8.99 (4)	15 (16)	16.92 (8)	-7.89 (33)	
<b>WR 30mm (1):</b>	3	1.75 (9)	18.52 (6)	18 (26)	31.60 (2)	-14.04 (7)	
<b>WR 30mm (2):</b>	3	1.46 (1)	21.54 (4)	20 (0)	32.33 (3)	-11.13 (3)	
<b>CSM 10mm (1)</b>	5	1.35 (4)	9.03 (7)	9 (21)	9.86 (4)	-1.03 (85)	
<b>CSM 10mm (2)</b>	2	1.30 (0)	7.63 (4)	9 (0)	10.00 (1)	-2.42 (3)	
<b>CSM 20mm (1)</b>	5	1.41 (16)	13.08 (11)	15 (19)	17.15 (1)	-4.18 (34)	
<b>CSM 30mm (1)</b>	5	1.50 (6)	21.85 (5)	20 (16)	30.65 (0)	-8.94 (8)	
<b>CSM 30mm (2)</b>	3	1.51 (5)	21.39 (3)	20 (12)	28.47 (2)	-7.47 (16)	

Table 1. Results summary (Numbers in parenthesis are % coefficients of variation)

Here there are two distinct sources of experimental variation: that *within* test series (i.e. between the individual tests of a test series performed within a relatively small area of a given panel), and that *between* tests series (each of which were performed on different parts of the same panel or on different nominally identical panels).

Table 1 shows that for the WR tests the variability of the Hertzian power law parameters within a test series is relatively low (e.g. Fig. 3), but that considerable variation was seen between nominally identical test series. This indicates that the indentation tests are very repeatable but that the characteristics of the hand laminated WR panels vary across the panel surface. Visual inspection of the panels indicates that the most influential characteristic here is the nature and thickness of the resin rich surface. This variability between test series is shown for the WR tests in Fig. 6.

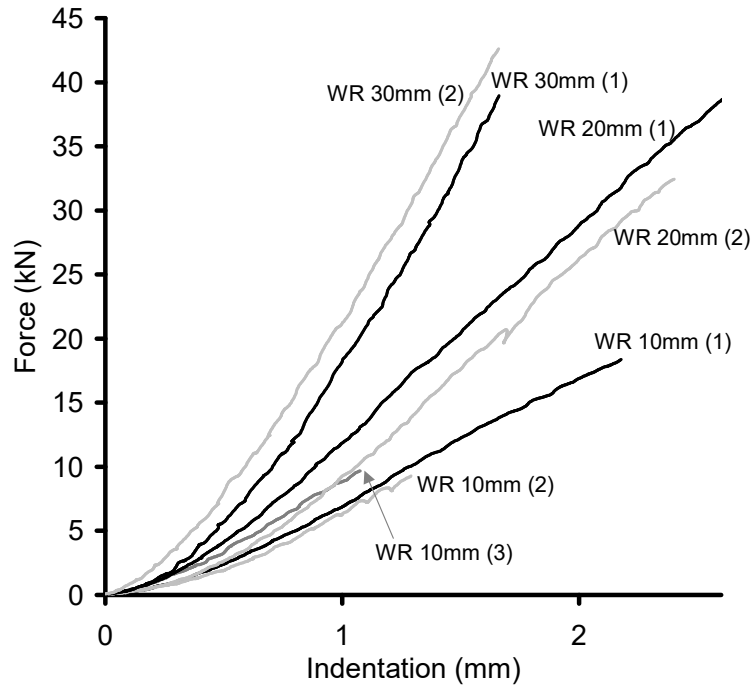


Fig. 6. Woven roving averaged contact responses.

Although the CSM panels also showed considerable variation across the panel surface, the Hertzian power law parameters given in Table 1 show much less variation between tests series, as illustrated in Fig. 7.

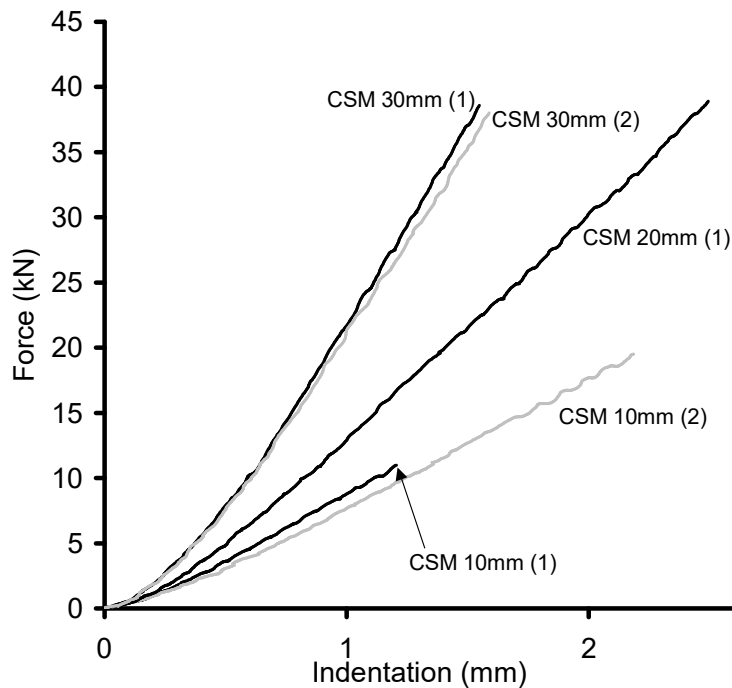


Fig. 7. Chopped strand mat averaged contact responses.

The slopes of the linear behaviour, however, show remarkably little variation between tests series for both WR and CSM laminates, and are also very similar for the two reinforcements. The modelling of this behaviour is beyond scope of this paper since it is thought to involve a

highly complex stress field together with complex and developing damage including delamination as well as matrix and fibre degradation. However, the slope appears to increase roughly linearly with the indenter radius. The linear intercept shows greater variation since this is dependent on the variability of both power law parameters and the transition load.

Comparing Fig. 6 with Fig. 7 shows that the contact responses of the CSM laminates lies at, or even slightly above the stiffest limit of the range of the equivalent WR responses. In Fig. 8 only the stiffest responses of each type of laminate at a given indenter diameter have been plotted to clarify this. This is unexpected given the significantly lower fibre content of the CSM composites. It may be postulated that this is because the random nature of the reinforcement fibres in the CSM laminate gives rise to more fibres lying in the z-plane, but further investigation would be needed to confirm this.

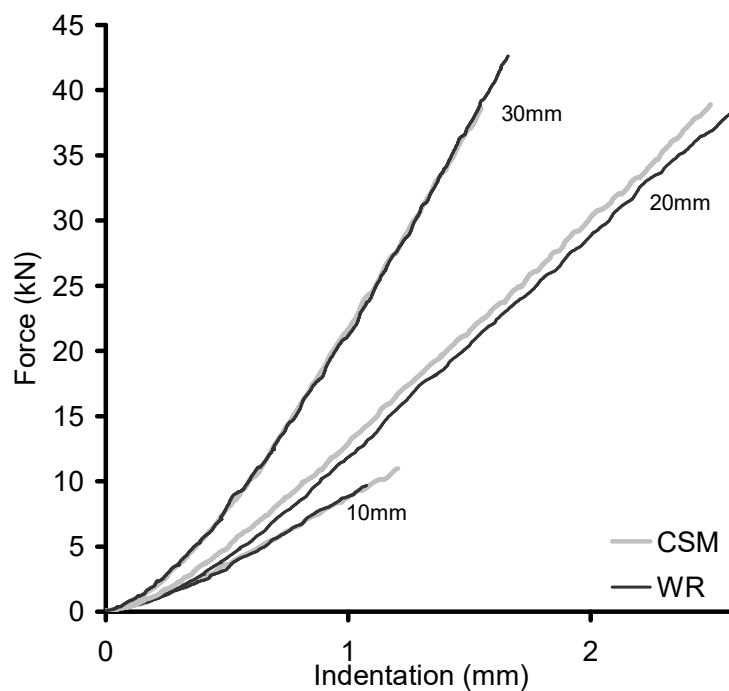


Fig. 8. Comparison of stiffest WR and CSM contact responses.

In both Eq. (4) and (6) the Hertzian contact stiffness coefficient  $n$  varies with the square root of indenter radius. However Fig. 9 shows that, although  $n$  does increase with indenter radius as expected, the variation of  $n^2$  with indenter radius is not linear as predicted.

A simple rule of mixtures approach [18] using the Young's modulus values for E-glass fibre and polyester matrix of 3.2 and 72 GPa respectively [18] gives the through thickness modulus of the 0.35 fibre volume fraction woven roving composite as 4.2 GPa. Although experimental values were not available to check this value, a similar approach for the longitudinal modulus (remembering that only half the fibres in a balanced woven roving are effective in the longitudinal direction) gave a value of 14 GPa, which was in extremely good agreement with the results of experimental flexural tests. Assuming a Young's modulus of the steel indenter of 200 GPa, and a Poisson's ratio of 0.3 both for composite and steel, Eq. (3) and (4) predict the values of  $n$  given in Table 2. Since in equation (3) the Poisson's

ratio of the composite is often taken as zero [7], predictions using this value are also included in Table 2.

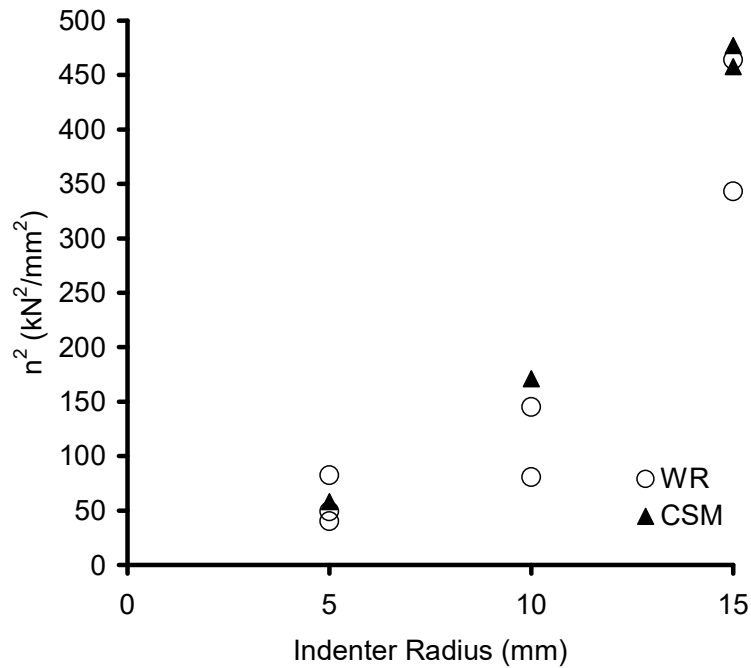


Fig. 9. Power law coefficient 'n' vs. indenter radius.

Indenter Radius (mm)	Theoretical n, ( $\nu_2=0.3$ ) (kN/mm <sup>3/2</sup> )	Theoretical n, ( $\nu_2=0$ ) (kN/mm <sup>3/2</sup> )	Experimental n (kN/mm <sup>3/2</sup> )
5	13	12	7-9
10	19	17	9-12
15	23	21	19-22

Table 2. Theoretical and experimental WR contact stiffness

The Hertzian contact stiffness is reasonably well predicted for the largest, 15 mm diameter indenter, but for the smaller 5 and 10 mm diameter indenters the experimental values are less than the predictions. The fact that the size of the weave is approaching the size of the smaller diameter indenters is thought to be significant, due to the unevenness of the woven surface.

If contact occurs at a 'peak' on the rough surface of the target of radius  $R_2$  (instead of the infinite radius of a flat surface) then Eq. (2) is used in place of equation (4) with a value of  $R$  which is less than that of  $R_1$ . This leads to a lower contact stiffness, as was seen experimentally and would be intuitively expected. Conversely, if contact occurs at a 'trough' on the surface then this will be in a resin rich area between rovings, similarly reducing the contact stiffness. A value of a zero Poisson's ratio for the composite target gives slightly better predictions than that of 0.3.

For the CSM laminates, the model for the through thickness modulus is not valid since it does not allow for fibres running in the through-thickness direction, and applicable data was not available in the literature. However, the fact that the Hertzian contact stiffness  $n$  values

were very similar for both materials suggests that, despite its lower fibre content, the through- thickness component of the fibre reinforcement of the CSM laminates leads to a similar through-thickness modulus to that of the WR laminates.

The transition load  $P_{trans}$  at which the contact stiffness became linear varied within a test series, but the average values were remarkably constant between test series for the same indenter diameter and even between woven roving and chopped strand mat tests. Assuming that the transition is due to internal delamination allows the substitution of  $P_{trans}$  for  $P_{crit}$  in Eq. (8). In Fig. 10 the square of the averaged  $P_{trans}$  values are plotted against the indenter radius. The strong linear relationship seen as predicted by Eq. (8), despite the fact that the actual stress distribution in these anisotropic materials is actually much more complex than assumed, further reinforces the deduction that the change to linear contact behaviour is due to the occurrence of internal delamination.

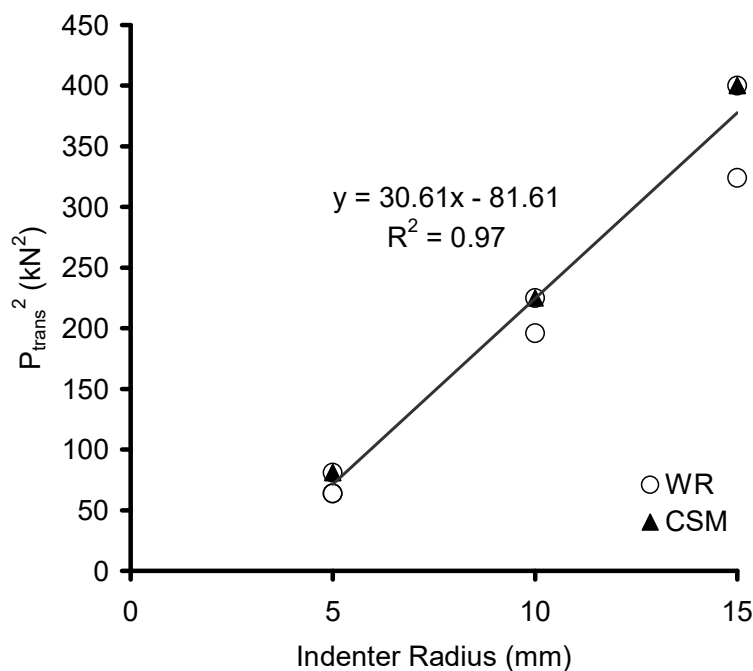


Fig. 10. Transition to linear contact response.

## 6. Conclusions

Quasi-static indentation tests on low fibre-volume, hand produced, E-glass/polyester ‘marine’ laminates have been performed. Hemispherical ended cylindrical indenters of diameters 10, 20 and 30 mm were used for both chopped strand mat and woven roving reinforced laminates.

A Hertzian contact law described well the initial response, and predicted the contact stiffness using the larger diameter indenter. The irregular woven roving surface was thought to be responsible for the lower contact stiffness than predicted seen for the smaller diameter indenters. Obtaining the power law parameters was extremely sensitive to the initial few data points, where the presence of an irregular resin-rich surface was influential.

At higher loads the response became linear as damage became significant. The transition to linear behaviour is thought to be due to delamination and was not sensitive to

reinforcement type. Good correlation of the transition load with indenter radius was obtained using a simplified shear delamination model. This contact induced delamination is thought to be significant in terms of the complex impact damage progression seen in co-current work.

The slope of the linear response increased approximately linearly with indenter radius, and was not sensitive to reinforcement type. The highly complex mechanisms responsible for this behaviour are thought to involve damage progression under a complex stress field and require further investigation.

Despite their significantly lower fibre-volume, chopped strand mat laminates exhibited a slightly higher contact stiffness than woven roving laminates.

The tests were very repeatable, but considerable material variability was seen in the Hertzian behaviour of the woven roving tests. To fully investigate the nature and sources of the variability a specifically designed statistical experimental investigation is required.

## Acknowledgment

The first author has been financed by Fundação para a Ciência e a Tecnologia, Lisbon, Portugal, under contract number SFRH/BPD/1568/2000.

## References

- [1] Sutherland L.S. and Guedes Soares C. Impact of low fibre-volume, glass / polyester rectangular plates. *Composites Structures* 2004 (in press).
- [2] Sutherland L.S. and Guedes Soares C. Impact characterisation of low fibre-volume glass reinforced polyester circular plates. *Int. J. Impact Eng.* 2004 (in press).
- [3] Abrate S. *Impact on composite structures*. Cambridge University Press, 1998.
- [4] Johnson K.L. *Contact mechanics*. Cambridge University Press, 1985.
- [5] Gladwell G.M.L. *Contact problems in the classical theory of elasticity*. Sijthoff and Noordhoff, 1980
- [6] Timoshenko S.P. and Goodier J.N. *Theory of elasticity*. McGraw-Hill, 1970.
- [7] Yang S.H. and Sun C.T. Indentation law for composite laminates. *ASTM STP 787*, 1982 p. 425-449
- [8] Tan T.M. and Sun C.T. Use of statical indentation laws in the impact analysis of laminated composite plates. *Trans. ASME* 1985;52:6-12.
- [9] Wu E. and Shyu K. Response of composite laminates to contact loads and relationship to low-velocity impact. *J. Composite Materials* 1993;27(15):1443-1464
- [10] Conway H.D. and Agnew Z. The pressure distribution between two elastic bodies in contact. *J. Mathematics and Physics* 1956;7:460-465.
- [11] Shivakumar K.N., Elber W. and Illg W. Prediction of impact force and duration due to low-velocity impact on circular composite laminates. *J. Appl. Mech.* 1985;52:674-680,.
- [12] Sankar B.V. An integral equation for the problem of smooth indentation of orthotropic beams. *Int. J. Solids Structures* 1989;25(3):327-337.

- [13] Sankar B.V. Smooth indentation of orthotropic beams. *Composites Sci. Technol.* 1989;34:95-111-
- [14] Keer L.M. and Ballarini R. Smooth indentation of an initially stressed orthotropic beam. *AIAA J.* 1983;21(7):1035-1042.
- [15] Cairns D.S. and Lagace P.A. Thick composite plates subjected to lateral loading. *J. Appl. Mechs.* 1987;14:611-616.
- [16] Wu E. And Yen C.S. The contact behaviour between laminated composite plates and rigid spheres. *J. Appl. Mechs.* 1994;61:60-66.
- [17] Mendenhall W. and Sincich T. *Statistics for Engineering and the Sciences.* Prentice Hall, 1995
- [18] Shenoj R.A. and Wellicome J.F. (eds.) *Composite Materials in Maritime Structures, Volume 1, Fundamental Aspects.* Cambridge University Press, 1993.